

# THE BIAS POTENTIAL AND PRESSURE NITROGEN EFFECT ON STRUCTURAL STRESS ON THE STRUCTURE-STRESSED STATE AND PROPERTIES OF NITRIDE COATINGS PRODUCED FROM HIGH-ENTROPY ALLOYS BY THE VACUUM ARC TECHNIQUE

*O.V. Sobol'<sup>2</sup>, A.A. Andreev<sup>2</sup>, V.N. Voevodin<sup>3</sup>, V.F. Gorban',  
S.N. Grigor'ev<sup>4</sup>, M.A. Volosova<sup>2</sup>, I.V. Serdyuk*

*National Technical University "KhPI, Kharkov, Ukraine;*

*<sup>2</sup>National Scientific Center «KIPT», Kharkov, Ukraine;*

*<sup>3</sup>Frantsevich Material Science Problem Institute, Kyiv, Ukraine;*

*<sup>4</sup>Moscow State Technological University "STANKIN", Moscow, Russia*

Experiments have been made to investigate the effect of negative bias potential and nitrogen atmosphere pressure on the structure-stressed state and properties of vacuum-arc nitride coatings. A comparison was made between the data for three groups of coatings: 1 – (Ti, V, Zr, Nb, Hf)N, 2 – (Ti, V, Zr, Nb, Hf, Ta)N and 3 – TiN. Without regard to the dropwise component, the multielement nitride coatings, deposited in the nitrogen atmosphere, represent a single-phase structure with a cubic fcc lattice (NaCl structure). At a substructural level in these coatings, the nitrogen pressure increase leads to an increase in crystallite sizes and to microstrain relaxation, whereas the increase in the bias potential results in the inverse effect (microstrain increase). In absolute magnitude, the microstrain in these coatings is higher, and the crystallite size is smaller than in the mononitride case. The highest hardness 70 GPa was attained with nitride coatings deposited by vacuum-arc evaporation of the (Ti, V, Zr, Nb, Hf) alloy at nitrogen pressure of 0.35 Pa.

## INTRODUCTION

The recently created multielement nitrides, as well as multilayered systems exhibit high mechanical properties [1-4]. Note that in this case one of the most important mechanical properties, in particular, hardness, is shown by nitrides of high-entropy alloys [5-14]. Among numerous systems having the highest hardness, we mention the heavy-element systems with a high binding energy of the components with nitrogen at nitride formation, and, in particular, the system based on Ti, V, Zr, Nb, Hf [15].

The aim of the present work has been to analyze the impact of the negative potential of the substrate and nitrogen atmosphere pressure on the structure-stressed state and hardness of nitrides produced from high-entropy alloys (Ti, V, Zr, Nb, Hf) and (Ti, V, Zr, Nb, Hf, Ta).

## METHODS OF SAMPLE PREPARATION AND EXAMINATION

The samples were obtained by means of vacuum-arc evaporation in the "Bulat-6" facility. The ingots of high-entropy five- (Ti, V, Zr, Nb, Hf) and six-element (Ti, V, Zr, Nb, Hf, Ta) alloys were produced by the method of vacuum-arc melting in high-purity argon atmosphere. Polished stainless steel (12Kh18N9T) plates, measuring 20x20x3 mm, as well as 0.2 mm thick copper foils were used as substrates. The coatings were deposited at a constant negative potential applied to the substrate  $U_b = -(50...200)$  V, an arc current of 85 A, residual gas pressure of 0.0066 Pa, nitrogen pressures ranging from 0.04 to 0.65 Pa. The deposition rate was determined to be about 4 nm/s.

Investigation into the structure-stressed state was performed with the diffractometer DRON-3M in the Cu-K $\alpha$  radiation. For monochromatization of the

registered radiation, a graphite monochromator was used, that was installed in the secondary beam (in front of the detector). The phase composition and the structure (texture, substructure) were investigated by traditional methods of X-ray diffractometry through the analysis of the position, intensity and form of diffraction reflection profiles. The diffractograms were interpreted with the use of the tables of the International Powder Diffraction File Center. The substructure characteristics were determined using the approximation technique [16]. For examination of the macro-stressed-strained state in the coatings having cubic (NaCl structure type) lattice, we have used the method of X-ray strain metering (" $\alpha$ -sin<sup>2</sup>  $\psi$ "-method). In the case of a strong texture, a modified " $\alpha$ -sin<sup>2</sup>  $\psi$ "-method" was used. It consisted in measuring interplanar spacings from different planes at certain crystallographically preset angles  $\psi$  of the sample inclination [17-18].

Microindentation was carried out at the "Micron-gamma" setup [19] at a load up to  $F = 0.5$  N by the Berkovich diamond pyramid having the cutting angle 65° with automatically alternated loading and unloading.

## RESULTS AND DISCUSSION

It is known that during deposition the negative bias potential supply to the substrate makes it possible to largely avoid the presence the drop-wise phase in the material formed [20-22]. In this case, with an increase in the negative bias potential up to – 200 V we attain an essential reduction in both the amount and the size of drops in the coating. The second important factor that exerts an effect on the structure and properties of vacuum-arc coatings is the working atmosphere pressure (nitrogen atmosphere  $P_N$  in case of nitride coatings formation).

The analysis of the measured X-ray diffraction spectra has shown that during deposition at nitrogen pressures ranging from 0.04 to 0.65 Pa, solid solution formation in the coatings takes place, based on the fcc lattice with nitrogen atoms implanted into octahedral interstitial sites (NaCl structure type).

For comparative analysis of the effect of the evaporated material composition on the phase-structural state of the coatings at different negative potential values, data correlation has been made for three groups of coatings: 1<sup>st</sup> group – coatings based on five-element (Ti, V, Zr, Nb, Hf) alloy nitride; 2<sup>nd</sup> group – coatings based on the nitride of six-element alloy (Ti, V, Zr, Nb, Hf, Ta); and 3<sup>rd</sup> group – TiN coatings. To deposit five-element coatings, we have used the alloy with the elements in the following ratio: Ti, V (light elements, 47...50 amu) – 40 at.%, Zr, Nb (medium-weight elements 91...92 amu) – about 45 at.%, and Hf (heavy elements, 178...180 amu) – about 15 at.%. To form six-element coatings, the alloy comprising six elements in the following ratios was used: Ti, V (light elements, 47...50 amu) – 20 at.%; Zr, Nb (medium-weight

elements, 91...92 amu) – about 45 at.%, and Hf, Ta (heavy elements, 178...180 amu) – about 35 at.%. So, in the first group the number of middle- and heavy-mass atoms approaches the number of light-mass atoms, while in the second group the number of middle- and heavy-mass atoms is four times higher than the number of light-mass atoms.

A comparison between the diffraction spectra of the coatings formed at the maximum nitrogen pressure (0.65 Pa) (Fig. 1) shows that all three coating groups are characterized by the development of the [111] texture. In the case of multielement alloys, a great width of reflections at  $\theta$ -scanning bears witness to a decreased degree of texture perfection as compared to the TiN case. Note that a high reflection intensity in the (Ti, V, Zr, Nb, Hf, Ta)N coating is determined by a high specific content of heavy components having a higher reflecting power.

At nitrogen pressure of 0.35 Pa, the (Ti, V, Zr, Nb, Hf)N coating spectrum shows a preferred crystallite orientation [220] (spectrum 2 in Fig. 2).

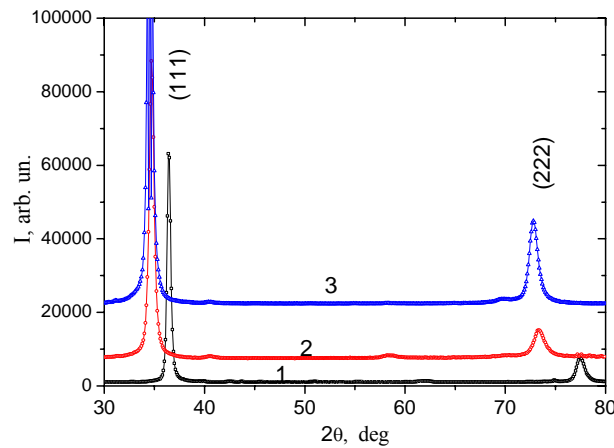


Fig. 1. Diffraction spectra regions of nitride coatings obtained at  $U_b = -200$  V and  $P_N = 0.65$  Pa. 1 – TiN; 2 – (Ti, V, Zr, Nb, Hf)N; 3 – (Ti, V, Zr, Nb, Hf, Ta)N

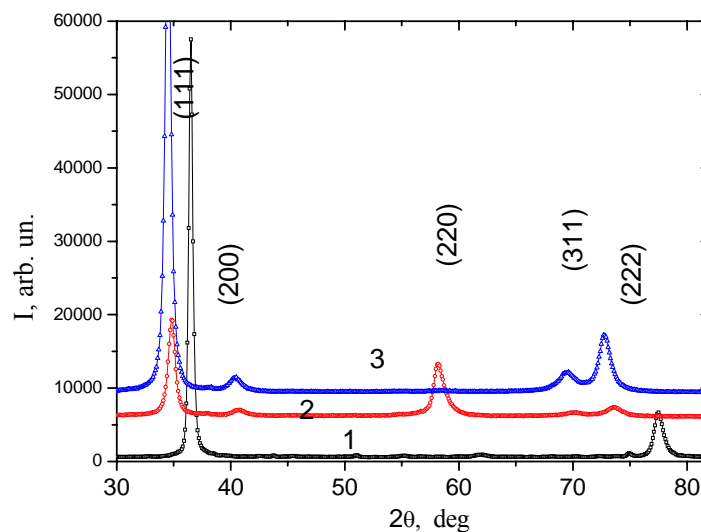


Fig. 2. Diffraction spectra regions of nitride coatings obtained at  $U_b = -200$  V and  $P_N = 0.35$  Pa. 1 – TiN; 2 – (Ti, V, Zr, Nb, Hf)N; 3 – (Ti, V, Zr, Nb, Hf, Ta)N

With a decrease in the nitrogen pressure down to 0.09 Pa, when in the plasma flow the concentration of metal ions and their average charge considerably increase [23], the effect of the radiation factor associated with the metal ion bombardment of the growing coating becomes dominant. That makes itself evident in intensification of the texture [220] in the (Ti, V, Zr, Nb, Hf)N coatings and in the appearance of the texture [311] in the (Ti, V, Zr, Nb, Hf, Ta)N coatings. It

should be noted here that on the coating surface there occurs the formation of a drop phase of two types: conical and spheroidal (Fig. 4). The composition of conical drops is characterized by a relatively low content of Ta (25...30 wt. %) and a higher content of Ti, Zr and Hf, while the composition of spheroidal drops is noted for their higher content of Ta and Nb. Table 1 lists the averaged values of drop compositions.

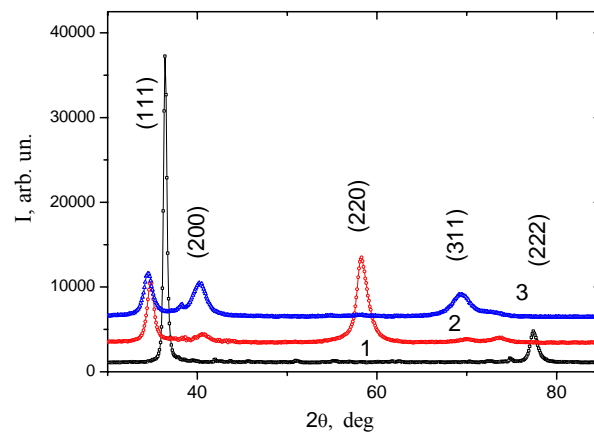


Fig. 3. Diffraction spectra regions of nitride coatings obtained at  $U_b = -200$  V and  $P_N = 0.09$  Pa. 1 – TiN; 2 – (Ti, V, Zr, Nb, Hf)N; 3 – (Ti, V, Zr, Nb, Hf, Ta)N

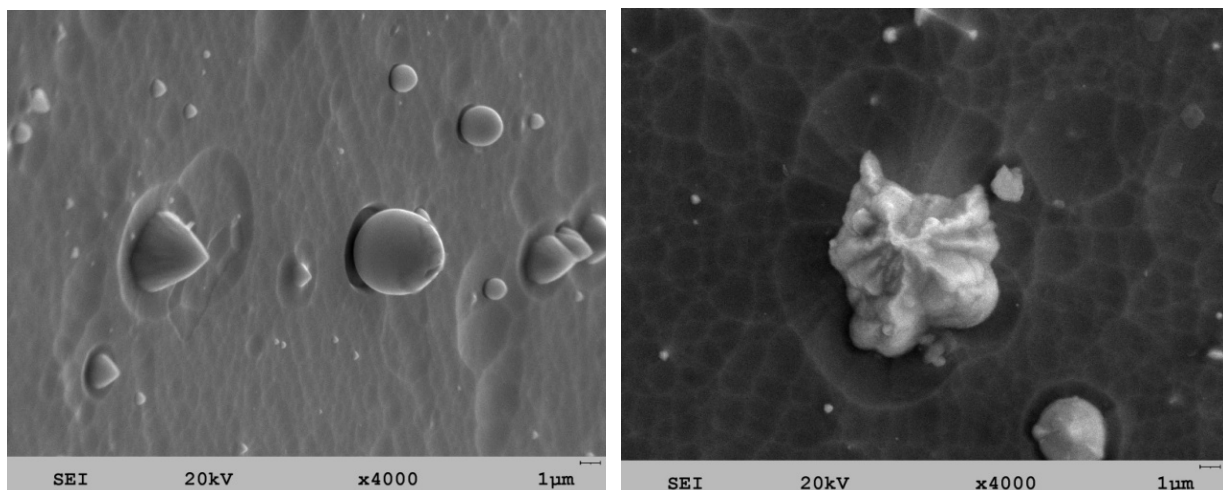


Fig. 4. Photomicrographs of six-element nitride coating surfaces formed at  $U_b = -00$  V,  $P_N = 0.35$  Pa. a – general appearance of the surface, b – partially sputtered drops

Drop compositions of the six-element coating (Ti, V, Zr, Nb, Hf, Ta)N

Table 1

Drop shapes	Ti	V	Zr	Nb	Hf	Ta
Conical	6.05	0.45	30.89	20.06	17.46	25.09
Spheroidal	3.31	0.61	12.66	28.61	8.49	46.33

The presence of two types of the drops may point to a local inhomogeneity of the cathode, and also, to the fact that the presence of tantalum in the drops substantially reduces their sputtering ratio.

With nitrogen pressure decrease down to 0.04 Pa, the action of the radiation factor at a shortage of

nitrogen atoms leads to the texture [311] increase in the coatings that have the highest specific content of heavy Ta component (Fig. 5, spectrum 3).

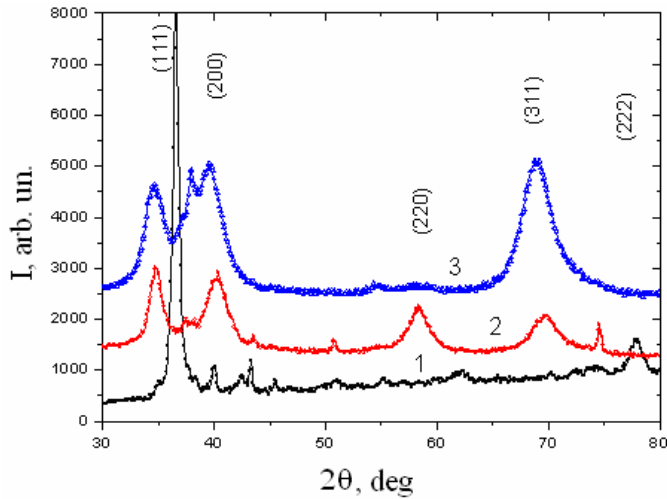


Fig. 5. Diffraction spectra regions of nitride coatings obtained at  $U_b = -200$  V and  $P_N = 0.04$  Pa.  
 1 – TiN; 2 – (Ti, V, Zr, Nb, Hf)<sub>3</sub>N;  
 3 – (Ti, V, Zr, Nb, Hf, Ta)<sub>3</sub>N

It should be noted that with decrease in  $U_b$  down to -100 V, the coatings under study exhibit no radiation effect on the texture formation (Fig. 6). The whole pressure range is characterized by the formation of the monotexture state with the preferred orientation [111] peculiar to the bias potential  $> -100$  V at vacuum-arc

deposition of mononitride coatings such as TiN, ZrN [24].

The data resulting from studies into substructure characteristics (crystallite size, microstrain) and obtained by the approximation technique [16], are generalized in Figs. 7 and 8.

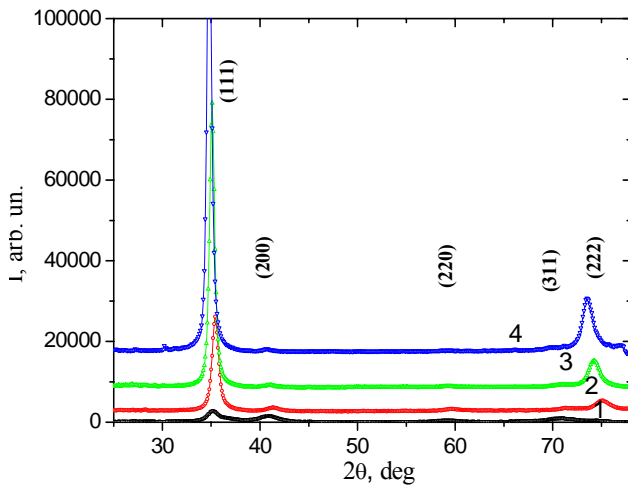


Fig. 6. Diffraction spectra regions of (Ti, V, Zr, Nb, Hf)<sub>3</sub>N coatings obtained at  $U_b = -100$  V and at nitrogen pressures  $P_N$ (Pa): 0.04(1); 0.09(2); 0.35 (3); 0.65 (4)

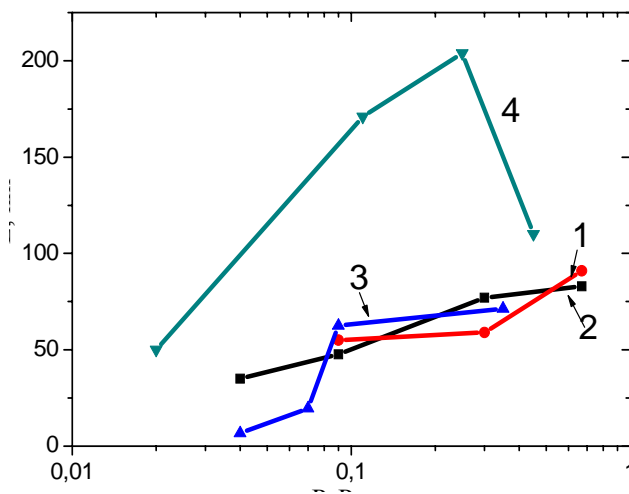


Fig. 7. Crystalline grain size versus nitrogen pressure for (Ti, V, Zr, Nb, Hf)<sub>3</sub>N coatings deposited at bias potentials of -100 V (1); -200 V (2); for (Ti, V, Zr, Nb, Hf, Ta)<sub>3</sub>N coatings deposited at  $U_b = -200$  V (3); TiN coatings deposited at  $U_b = -200$  V (4)

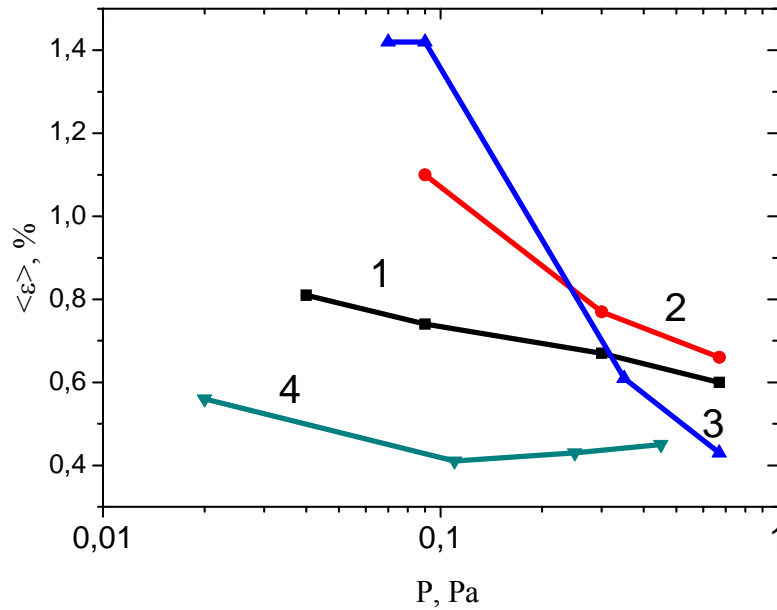


Fig. 8. Microstrain versus nitrogen pressure for (Ti, V, Zr, Nb, Hf)N coatings deposited at bias potentials of -100 V (1); -200 V (2); for (Ti, V, Zr, Nb, Hf, Ta)N coatings deposited at  $U_b = -200$  V (3); TiN coatings deposited at  $U_b = -200$  V (4)

It can be seen that in contrast to TiN coatings, in the case of multielement nitride coatings the average crystalline grain size decreases, while the microstrain increases. In particular, this is typical for the (Ti, V, Zr, Nb, Hf, Ta)N coatings (see lines 3 in Figs. 7 and 8). The increase in the microstrained state due to the difference in atomic radii of the components leads to the decrease in the crystalline grain size. Besides, a considerable increase in the microstrain and the decrease in the average crystallite size are observed as the pressure gets reduced. This is caused by the formation of the defect structure on the coating surface having a great number of crystallization centers due to the increase in the concentration of ions and their average charge in the plasma [23]. In comparison with the TiN coatings, the high-entropy alloy nitride (HEAN) coatings have a substantially smaller average size of crystallites at the same nitrogen pressures (see Fig. 7). The introduction of the sixth heavy element (Ta) leads to a decrease in the average crystalline grain size, this being particularly noticeable at low pressures.

It can be seen (Fig. 8) that the highest microstrain is peculiar to the (Ti, V, Zr, Nb, Hf, Ta)N coatings (curve 3) deposited at low nitrogen pressures. This is due to the difference in atomic radii of the components. At a low pressure, owing to the increase in the average charge, their ions are implanted into the coating with a higher energy. Thus, in the (Ti, V, Zr, Nb, Hf)N coatings the maximum strain value changes from 0.8% at -100 V up to 1.1% at -200 V. In the (Ti, V, Zr, Nb, Hf, Ta)N coatings the microstrain value is higher and attains 1.42% at  $U_b = -200$  V (curve 3).

With an increasing nitrogen pressure, when the deposited particle energy decreases, all the coatings display reduction in the microstrain.

A comparison with the corresponding parameters for TiN coatings (see curve 4 in Fig. 8) shows that the microstrain developing in TiN coatings is substantially lower in its absolute value, and only at high pressures and oversaturation with nitrogen atoms it becomes comparable with that of multielement nitrides.

The stress-strain state analysis performed by the method of multiple inclined exposures (" $\alpha$ - $\sin^2\psi$ " method) has demonstrated that for both the (Ti, V, Zr, Nb, Hf)N and (Ti, V, Zr, Nb, Hf, Ta)N coatings an increase in the nitrogen pressure leads to an increase in the negative angle of plots inclination, that points to the development of a greater compression strain. The characteristic feature of the HEAN coatings is the intersection of the plots at the point, for which  $\sin^2\psi \approx 0.4$ . In the cubic lattice case, this intersection corresponds to the Poisson ratio  $\mu$  close to 0.25 ( $\sin^2\psi_0 = 2\mu/(1+\mu)$  [25]), this being characteristic of the nitrides with a strong covalent bond between the metal and nitrogen, e.g., TiN. The increase in the lattice spacing at  $\sin^2\psi_0 = 0.4$  from 0.44294 nm in the (Ti, V, Zr, Nb, Hf)N coating up to 0.44485 nm in the (Ti, V, Zr, Nb, Hf, Ta)N coating is attributed to the increase in the content of metallic constituents having a larger atomic radius: Hf and Ta.

The investigation of such a universal characteristic of the mechanical properties of coatings as the hardness has shown (Fig. 9) that for the HEAN coatings under discussion the highest hardness is attained at a pressure of 0.35 Pa. At this pressure, on the one part, we have a rather high compressive stress-strain state in the coatings, and on the other part, the ratio between the metal atoms and nitrogen atoms is close to equiatomic.

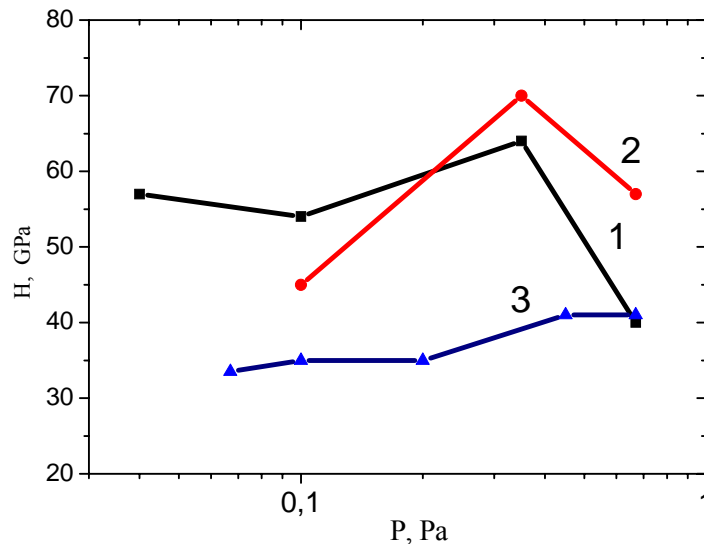


Fig. 9. Microhardness versus nitrogen pressure at the potential  $-200$  V: 1 –  $(\text{Ti}, \text{V}, \text{Zr}, \text{Nb}, \text{Hf})\text{N}$  coatings; 2 –  $(\text{Ti}, \text{V}, \text{Zr}, \text{Nb}, \text{Hf}, \text{Ta})\text{N}$  coatings; 3 –  $\text{TiN}$  coatings

A comparison with  $\text{TiN}$  coatings formed at  $U_b = -200$  V shows that the hardness of nitride coatings produced from five- and six-element alloys is considerably higher in absolute values than that of  $\text{TiN}$  (see curve 3, Fig. 9).

It can be seen that the highest hardness is exhibited by the coatings produced at a pressure of 0.35 Pa. Furthermore, a higher hardness of multielement nitride coatings owes to a strong microstrain in crystallites due to the presence there of the components having different atomic radii; that stimulates the formation of a finer crystalline nanostructure.

## CONCLUSIONS

Without regard for the dropwise component, the HEAN coatings deposited in the nitrogen atmosphere have a single-phase structure with a cubic fcc lattice ( $\text{NaCl}$ -type structure).

The supply of bias potential  $U_b = -200$  V to the substrate results in the formation of a radiation-stimulated texture with the  $[110]$  axis in the  $(\text{Ti}, \text{V}, \text{Zr}, \text{Nb}, \text{Hf})\text{N}$  coatings, for which the content of light metal components ( $\text{Ti}, \text{V}$ ) considerably exceeds the content of heavy components ( $\text{Hf}$ ), as well as the texture with the  $[311]$  axis in the  $(\text{Ti}, \text{V}, \text{Zr}, \text{Nb}, \text{Hf}, \text{Ta})\text{N}$  coatings, for which the content of light metal components ( $\text{Ti}, \text{V}$ ) is comparable with the content of heavy components ( $\text{Hf}, \text{Ta}$ ).

The HEAN coatings deposited at the highest pressure of 0.65 Pa exhibit the texture with the  $[111]$  axis perpendicular to the growth surface.

The Poisson ratio of nitride coatings deposited from high-entropy alloys has been found to be about 0.25, this being typical for mononitrides having a strong  $\text{Me-N}$  bond.

At the substructural level, in the HEAN coatings an increase in the nitrogen pressure leads to an increase in the crystalline grain size and to microstrain relaxation. The microstrain in these coatings is higher in its absolute value than that of mononitrides. This is due to the fact that the crystal lattice of HEAN coatings

comprises several elements that have substantially different atomic radii.

In the pressure range 0.04...0.4 Pa increasing bias potential leads to both a growth of microstrain and a decrease in the average size of crystallites in the HEAN coatings. At the highest size of pressure of 0.65 Pa, as the bias potential  $U_b$  increases, the crystallite size also increases.

The highest hardness attains 70 GPa in the  $(\text{Ti}, \text{V}, \text{Zr}, \text{Nb}, \text{Hf})\text{N}$  coatings at a nitrogen pressure of 0.35 Pa. The special features of this state are: 1) the bitexture state, 2) the composition close to stoichiometric composition in relation to nitrogen, 3) the average crystalline grain size of about 40 nm.

## REFERENCES

1. *Nanostructured coatings*. Edited by: Cavaleiro, Albano; De Hosson, Jeff Th. M. Springer-Verlag, 2006, 648 p.
2. N.A. Azarenkov, O.V. Sobol', A.D. Pogrebnyak, V.M. Beresnev. *Vacuum-arc coating engineering*. Kharkov: V. Karazin KhNU Publishers, 2011, 344 p. (in Russian)
3. A.D. Pogrebnyak, A.P. Shpak, N.A. Azarenkov, and V.M. Beresnev. Structures and properties of hard and superhard nanocomposite coatings // *Physics-Uspekhi*. 2009, v. 52, N 1, p. 29-54.
4. O.V. Sobol', A.A. Andreyev, S.N. Grigoriev, et al. Vacuum-arc multilayer nanostructured  $\text{TiN/Ti}$  coatings: structure, stress state, properties // *Metal Science and Heat Treatment*. 2012, v. 54, issue 1-2, p. 28-33.
5. T.K. Chen, T.T. Shun, J.W. Yeh, M.S. Wong // *Surf. Coat. Technol.* 2004, v. 188-189, p. 193.
6. V. Dolique, A.L. Thomann, P. Brault, Y. Tessier, P. Gillon // *Surf. Coat. Technol.* 2010, v. 204, p. 1989.
7. C.H. Lai, S.J. Lin, J.W. Yeh, S.Y. Chang // *Surf. Coat. Technol.* 2006, v. 200, p. 3275.
8. C.H. Lin, J.G. Duh, J.W. Yeh. *Surf. Coat. Technol.* 2007, v. 201, p. 6304.

9. H.W. Chang, P.K. Huang, A. Davison, J.W. Yeh, C.H. Tsau, C.C. Yang // *Thin Solid Films*. 2008, v. 516, p. 6402.
10. M.H. Tsai, C.H. Lai, J.W. Yeh, J.Y. Gan // *J. Phys. D*. 2008, v. 41, p. 235402-1.
11. P.K. Huang, J.W. Yeh // *Surf. Coat. Technol.* 2009, v. 203, p. 1891.
12. D.C. Tsai, Y.L. Huang, S.R. Lin, S.C. Liang, F.S. Shieu // *Appl. Surf. Sci.* 2010, v. 256, p. 1361.
13. S.C. Liang, Z.C. Chang, D.C. Tsai, Y.C. Lin, H.S. Sung, M.J. Deng, F.S. Shieu // *Appl. Surf. Sci.* 2011, v. 257, p. 7709.
14. M. Braic, V. Braic, M. Balaceanu, C.N. Zoita, A. Vladescu, E. Grigore // *Surf. Coat. Technol.* 2010, v. 204, p. 2010
15. O.V. Sobol', A.A. Andreyev, V.F. Gorban', N.A. Krapivka, V.A. Stolbovoi, I.V. Serdyuk, V.E. Fil'chikov. Reproducibility of the single-phase structural state of the multielement high-Nb entropy Ti-V-Zr-Nb-Hf system and related superhard nitrides formed by the vacuum-arc method // *Technical Physics Letters*. 2012, v. 38, N 7, p. 616-619.
16. L.S. Palatnik, M.Ya. Fuks, V.M. Kosevich. *The formation mechanism and substructure of condensed films. M.: Nauka publ.*. 1972, 320 p. (in Russian).
17. I.C. Noyan, J.B. Cohen. *Residual Stress Measurement by Diffraction and Interpretation*. New York: Springer-Verlag, 1987, 350 p.
18. C. Genzel, W. Reinmers. A Study of X-ray Residual-Stress Gradient Analysis in Thin-Layers with Strong Filer Texture // *Phys. Stat. Solidi: A-Applied Research*. 1998, v. 166, №2, p. 751-762.
19. E. Aznakayev. *Proceedings of the International Conference "Small Talk-2003"*, San Diego, California, USA, TP.001. 2003, p. 8.
20. A.A. Andreyev, L.P. Sablev, S.N. Grigoriev. *Vacuum-arc coatings*. Kharkov: NSC KIPT, 2010, 317 p. (in Russian).
21. O.V. Sobol', A.D. Pogrebnyak, V.M. Beresnev. Effect of the Preparation Conditions on the Phase Composition, Structure, and Mechanical Characteristics of Vacuum-Arc Zr-Ti-Si-N Coatings // *Physics of Metals and Metallography*. 2011, v. 112:2, p. 188-195.
22. O.V. Sobol', A.A. Andreev, S.N. Grigoriv, et al. Effect of high-voltage pulses on the structure and properties of titanium nitride vacuum-arc coatings // *Metal science and heat treatment*. 2012, v. 54, issue 3-4, p. 195-205.
23. I.I. Aksonov. *Vacuum arc in erosive plasma sources*. Kharkov: NSC KIPT, 2005, 211 p. (in Russian).
24. N.A. Azarenkov, O.V. Sobol, A.D. Pogrebnyak, V.M. Beresnev, S.V. Lytovchenko, O.N. Ivanov. Materialovedenie neravnovesnogo sostoyania modifitsirovannoy poverhnosti // *The materials science of non-equilibrium states of modified surface*. Sumy: Sumy State University, 2012, 683 p.
25. O.V. Sobol'. Control of the Structure and Stress State of thin films and coatings in the process of their preparation by ion-plasma methods // *Physics of the Solid State*. 2011, v. 53, №7, p. 1464-1473.

Article received 13.11.2013

**ВЛИЯНИЕ ПОТЕНЦИАЛА СМЕЩЕНИЯ И ДАВЛЕНИЯ АЗОТА НА СТРУКТУРНО-НАПРЯЖЕННОЕ СОСТОЯНИЕ И СВОЙСТВА НИТРИДНЫХ ПОКРЫТИЙ, ПОЛУЧЕННЫХ ИСПАРЕНИЕМ ВЫСОКОЭНТРОПИЙНЫХ СПЛАВОВ ВАКУУМНО-ДУГОВЫМ МЕТОДОМ**

*О.В. Соболев, А.А. Андреев, В.Н. Воеводин, В.Ф. Горбань, С.Н. Григорьев, М.А. Волосова, И.В. Сердюк*

Проведено исследование влияния отрицательного потенциала смещения и давления атмосферы азота на структурно-напряженное состояние и свойства вакуумно-дуговых нитридных покрытий. Проведено сопоставление данных по трем группам покрытий: 1 – (Ti, V, Zr, Nb, Hf)N, 2 – (Ti, V, Zr, Nb, Hf, Ta)N и 3 – TiN. Без учета капельной составляющей многоэлементные нитридные покрытия, осажденные в азоте, являются однофазными с кубической ГЦК-решеткой (структурный тип NaCl). На субструктурном уровне в этих покрытиях повышение давления азота приводит к увеличению размеров кристаллитов и релаксации микродеформации, а повышение потенциала смещения – к обратному эффекту (увеличение микродеформации). По абсолютной величине микродеформация в таких покрытиях выше, а размер кристаллитов – меньше, чем для моонитридов. Наибольшая твердость 70 ГПа достигнута в нитридных покрытиях, осажденных вакуумно-дуговым испарением (Ti, V, Zr, Nb, Hf) сплава при давлении азота 0,35 Па.

**ВПЛИВ ПОТЕНЦІАЛУ ЗСУВУ ТА ТИСКУ АЗОТУ НА СТРУКТУРНО-НАПРУЖЕНИЙ СТАН І ВЛАСТИВОСТІ НІТРИДНИХ ПОКРИТТІВ, ОТРИМАНИХ ВИПАРУВАННЯМ ВИСОКОЕНТРОПІЙНИХ СПЛАВІВ ВАКУУМНО-ДУГОВИМ МЕТОДОМ**

*О.В. Соболев, А.А. Андреев, В.М. Воеводин, В.Ф. Горбань, С.Н. Григорьев, М.О. Волосова, И.В. Сердюк*

Проведено дослідження впливу негативного потенціалу зсуву і тиску азоту на структурно-напружений стан і властивості вакуумно-дугових нітридних покриттів. Проведено порівняння даних за трьома групами покриттів: 1 – (Ti, V, Zr, Nb, Hf)N, 2 – (Ti, V, Zr, Nb, Hf, Ta)N і 3 – TiN. Без урахування крапельної складової багатоелементні нітридні покриття, нанесені в азоті, є однофазними з кубічними ГЦК-ґратками (структурний тип NaCl). На субструктурному рівні в цих покриттях підвищення тиску азоту призводить до збільшення розмірів кристалітів і релаксації мікродеформації, а підвищення потенціалу зсуву – до зворотного ефекту. За абсолютною величиною мікродеформації в таких покриттях вища, а розмір кристалітів – менше, ніж для моонітриду. Найбільша твердість 70 ГПа досягнута в нітридних покриттях, нанесених вакуумно-дуговым випаруванням (Ti, V, Zr, Nb, Hf) сплаву при тиску азоту 0,35 Па.